Inter-carrier Interference Reduction Scheme for SFBC-OFDM Systems

Kyung-Hwa Kim and Bangwon Seo

In this paper, we first analyze carrier-to-interference ratio performance of the space–frequency block coded orthogonal frequency-division multiplexing (SFBC-OFDM) system in the presence of phase noise (PHN) and residual carrier frequency offset (RCFO). From the analysis, we observe that conventional SFBC-OFDM systems suffer severely in the presence of PHN and RCFO. Therefore, we propose a new inter-carrier interference (ICI) self-cancellation method — namely, ISC — for SFBC-OFDM systems to reduce the ICI caused by PHN and RCFO. Through the simulation results, we show that the proposed scheme compensates the ICI caused by PHN and RCFO in Alamouti SFBC-OFDM systems and has a better performance than conventional schemes.

Keywords: Inter-carrier interference, SFBC, OFDM, self-cancellation.

I. Introduction

Orthogonal frequency-division multiplexing (OFDM) is the most widely used multi-carrier modulation scheme. It is used in communication systems, such as Digital Audio Broadcasting [1], Digital Video Broadcasting [2], and asymmetric digital subscriber line [3], as well as appearing in the IEEE 802.11a amendment to the IEEE 802.11 specification [4]. It has been considered as a promising candidate for broadband wireless communication systems because of its high data rate, high spectral efficiency, and robustness to the frequency-selective channel [5].

On the other hand, space–frequency block code (SFBC) exploits both spatial- and frequency-diversity gain. To take advantage of the desirable properties of both OFDM and SFBC, a combination of these two techniques has been proposed in [6]–[8]. When the Alamouti SFBC codeword [9] is transmitted through adjacent OFDM subcarriers in the same OFDM symbol, this combined system is known as an Alamouti SFBC-OFDM system.

The main drawback of the OFDM-based systems is that they are too sensitive to phase noise (PHN), introduced by the local oscillator, and to residual carrier frequency offset (RCFO). The PHN and RCFO destroy the orthogonality among subcarriers and introduce inter-carrier interference (ICI), which degrades the performance of OFDM-based systems. The effects of PHN and RCFO on OFDM systems have been studied by several authors [10]–[12]. The two main effects of PHN and RCFO on OFDM systems are common phase error (CPE) and ICI. CPE causes phase rotation in subcarriers. This phase rotation is constant in all subcarriers and can be corrected through the use of pilot-symbol assisted phase estimation. On the contrary, it is impossible to completely eliminate ICI.

Manuscript received July 17, 2013; revised Dec. 4, 2013; accepted Mar. 18, 2014.

This research was supported by the International Science and Business Belt Program through the Ministry of Science, ICT and Future Planning (former Education, Science and Technology) (2013K000490).

Kyung-Hwa Kim (khwa@kaist.ac.kr) is with LG Electronics, Seoul, Rep. of Korea.

Bangwon Seo (corresponding author, seobw@kongju.ac.kr) is with the Division of Electrical, Electronic and Control Engineering, Kongju National University, Cheonan, Rep. of Korea.

Among several PHN compensation schemes [13]–[18], the ICI self-cancellation (ISC) method has received much attention because of its simplicity. The main idea of this method is to map one data symbol onto a group of subcarriers by considering the predefined ICI weighting function. By doing so, ICI signals generated within a group can self-cancel each other via a simple method [13]–[15]. We note that the idea of mapping one data symbol onto a group of subcarriers has also been used in multiband OFDM systems to obtain frequency diversity gain [19]–[20]. This notion is the underlying essence of the dual carrier modulation (DCM) scheme. However, since each data symbol in a DCM scheme is mapped onto two subcarriers with the same frequency separation and without considering the ICI, the DCM scheme cannot reduce the ICI caused by PHN and RCFO.

Among the conventional ISC schemes, a symmetric data-conjugated ISC scheme [15], in short, symmetric ISC hereafter, utilized the symmetric conjugate property of the ICI weighting function and showed the best carrier-to-interference ratio (CIR) and bit error rate (BER) performance. However, the performance of the symmetric ISC method degrades severely when the normalized 3 dB bandwidth (ρ) of the PHN is large or there exists RCFO.

In this paper, we propose a new ISC method for SFBC-OFDM systems to improve the BER performance when $\rho \geq 1$ or there exists RCFO. In the proposed scheme, owing to a new interference cancellation mapping at the transmitter, time-domain transmit signals become real values after an inverse discrete Fourier transform (IDFT). By using the real property of the transmitted signal, PHN and RCFO are blindly estimated and compensated at the receiver; therefore, ICI can be reduced much more in the proposed scheme compared with the conventional ISC method. A theoretical CIR expression of the proposed scheme is derived based on the symmetric conjugate property of the ICI weighting function of the PHN. The CIR and BER performance of the proposed scheme is compared with those of the conventional schemes.

The rest of this paper is organized as follows. In Section II, we describe the system model. In Section III, we propose a new ISC method for SFBC-OFDM systems and derive the CIR performance of the proposed scheme. In Section IV, we present our simulation results, and in Section V, we conclude the paper.

II. System Model and Problem Formulation

Figure 1 shows a conventional SFBC-OFDM system applying Alamouti code in the frequency domain. Let $S_{k,i}$ denote the data symbol transmitted from the ith transmit antenna on the kth subcarrier. Consider two adjacent subcarriers, say k and k+1, where k is an even number. For subcarrier k, $S_{k,1} = X_k$ and $S_{k,2} = -X^*_{k+1}$ are transmitted from transmit antenna 1 (TX1) and transmit antenna 2 (TX2), respectively. For subcarrier k+1, $S_{k+1,1} = X_{k+1}$ and $S_{k+1,2} = X^*_k$ are transmitted from TX1 and TX2, respectively, where $(\cdot)^*$ stands for the conjugate operation and X_k is the kth information data with the following property:

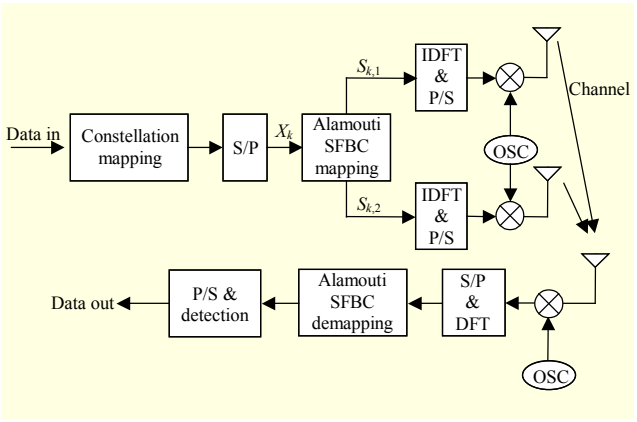

Fig. 1. Block diagram of conventional Alamouti SFBC-OFDM system.

$$E[X_k X_l^*] = \begin{cases} E[|X_k|^2] = 1 & k = l, \\ 0 & k \neq l. \end{cases} \quad (1)$$

When there exist PHN ϕ_n and RCFO ε, the received signal is affected by PHN and RCFO and can be written as

$$Y_k = H_{k,1} X_k \Theta_{-\varepsilon} - H_{k,2} X^*_{k+1} \Theta_{-\varepsilon} + I_{k,1} + I_{k,2} + W_k, \quad (2)$$

$$Y_{k+1} = H_{k+1,1} X_{k+1} \Theta_{-\varepsilon} + H_{k+1,2} X^*_k \Theta_{-\varepsilon} + I_{k+1,1} + I_{k+1,2} + W_{k+1}, \quad (3)$$

where $H_{k,i}$, i = 1, 2, denotes a frequency-domain channel response for the kth subcarrier of the ith transmit antenna and W_k is a frequency-domain additive white Gaussian noise (AWGN) in the subcarrier k. The term $I_{k,u}$, u = 1, 2, means the inter-carrier interference from the uth TX and is expressed by

$$I_{k,1} = \sum_{\substack{m=0 \\ m \neq k}}^{N-1} H_{m,1} X_m \Theta_{k-m-\varepsilon}, \quad (4)$$

$$I_{k,2} = -\sum_{\substack{m=0,2,4,\ldots \\ m \neq k}}^{N-2} H_{m,2} X^*_{m+1} \Theta_{k-m-\varepsilon} + \sum_{\substack{m=1,3,5,\ldots \\ m \neq k}}^{N-1} H_{m,2} X^*_{m-1} \Theta_{k-m-\varepsilon}, \quad (5)$$

where N is the total number of subcarriers, and the term $\Theta_{k-\varepsilon}$ is an ICI weighting function of the kth subcarrier in the presence of RCFO, ε, which is given by

$$\Theta_{k-\varepsilon} = \frac{1}{N} \sum_{n=0}^{N-1} e^{j\phi_n} e^{-j2\pi n(k-\varepsilon)/N}. \quad (6)$$

http://dx.doi.org/10.4218/etrij.14.0113.0711

To focus on the influence of PHN, we consider only quasi-static and flat channels; thus, the frequency response of a channel will always be equal to one (that is, $H_{m,1} = H_{m,2} = 1$) [15]. The effect of the channel coefficients will be considered in Section V.

In the conventional de-mapping block for Alamouti SFBC-OFDM systems, the decision variables $\hat{X}_k$ and $\hat{X}_{k+1}$ for $k = 0, 2, 4, \ldots, N-2$, are given by [15]

$$\begin{aligned}\hat{X}_k &= \frac{Y_k + Y_{k+1}^*}{2} \\ &= \frac{1}{2}(\Theta_{-\varepsilon} + \Theta_{-\varepsilon}^*)X_k - \frac{1}{2}(\Theta_{-\varepsilon} - \Theta_{-\varepsilon}^*)X_{k+1}^* \\ &\quad + \frac{I_{k,1} + I_{k+1,1}^* + I_{k,2} + I_{k+1,2}^*}{2} + \frac{W_k + W_{k+1}^*}{2}\end{aligned} \tag{7}$$

and

$$\begin{aligned}\hat{X}_{k+1} &= \frac{Y_{k+1} - Y_k^*}{2} \\ &= \frac{1}{2}(\Theta_{-\varepsilon} + \Theta_{-\varepsilon}^*)X_{k+1} + \frac{1}{2}(\Theta_{-\varepsilon} - \Theta_{-\varepsilon}^*)X_k^* \\ &\quad + \frac{I_{k+1,1} - I_{k,1}^* + I_{k+1,2} - I_{k,2}^*}{2} + \frac{W_{k+1} - W_k^*}{2}.\end{aligned} \tag{8}$$

From (7) and (8), we can observe that PHN and RCFO introduce ICI among subcarriers in an OFDM symbol in addition to the interference between TXs. Therefore, the orthogonality property of the Alamouti SFBC is destroyed, which reduces the diversity gain and causes an error floor in the high-SNR region [21]. Therefore, ICI has to be effectively suppressed in Alamouti SFBC-OFDM systems to achieve a better BER performance than that of OFDM systems with a single transmit antenna.

The ICI power of the Alamouti SFBC-OFDM system at the 0th subcarrier can be easily shown to be

$$ICI_{\text{SFBC}} = \frac{1}{4}E\left[\left|(\Theta_{-\varepsilon} + \Theta_{-\varepsilon}^*)X_1^* + I_{0,1} + I_{1,1}^* + I_{0,2} + I_{1,2}^*\right|^2\right]. \tag{9}$$

This can be rewritten as

$$ICI_{\text{SFBC}} = \sum_{m=1}^{N-1} |\Theta_{-m-\varepsilon}|^2 + \frac{1}{4}|\Theta_{-\varepsilon} - \Theta_{-\varepsilon}^*|^2. \tag{10}$$

The derivation of (10) is given in the Appendix.

For comparison, the ICI power at the 0th subcarrier in single-input–single-output (SISO)-OFDM systems can be represented as follows [15]:

$$ICI_{\text{SISO}} = \sum_{m=1}^{N-1} |\Theta_{-m-\varepsilon}|^2. \tag{11}$$

Therefore, the ICI power in SFBC-OFDM systems is increased by as much as $|\Theta_{-\varepsilon} - \Theta_{-\varepsilon}^*|^2/4$ compared with the ICI power in SISO OFDM systems. If there is no RCFO ($\varepsilon = 0$) and the standard deviation (STD) of the PHN is small, then we obtain $|\Theta_{-\varepsilon} - \Theta_{-\varepsilon}^*|^2 \approx 0$ and the BER performance of Alamouti SFBC-OFDM systems is better than that of SISO-OFDM systems due to the diversity gain.

The CIR at the 0th subcarrier in conventional SFBC-OFDM systems can be expressed as

$$\begin{aligned}CIR_{\text{SFBC}} &= \frac{E[|(\Theta_{-\varepsilon} + \Theta_{-\varepsilon}^*)X_0|^2]/4}{ICI_{\text{SFBC}}} \\ &= \frac{|\Theta_{-\varepsilon} + \Theta_{-\varepsilon}^*|^2/4}{\sum_{m=1}^{N-1} |\Theta_{-m-\varepsilon}|^2 + |\Theta_{-\varepsilon} - \Theta_{-\varepsilon}^*|^2/4}.\end{aligned} \tag{12}$$

The CIR at the 0th subcarrier in SISO-OFDM systems is given by [15]

$$\begin{aligned}CIR_{\text{SISO}} &= \frac{E[|X_0\Theta_{-\varepsilon}|^2]}{E[|\sum_{m=1}^{N-1} X_m\Theta_{-m-\varepsilon}|^2]} \\ &= \frac{|\Theta_{-\varepsilon}|^2}{\sum_{m=1}^{N-1} |\Theta_{-m-\varepsilon}|^2}.\end{aligned} \tag{13}$$

By comparing (12) and (13), we can observe that $CIR_{\text{SFBC}} \le CIR_{\text{SISO}}$.

Figure 2 shows scatter diagrams of the quadrature phase-shift keying (QPSK) constellation as a function of the STD of PHN (ρ) for a SISO-OFDM system and a conventional Alamouti SFBC-OFDM system, to compare the effect of PHN where AWGN was not considered and N = 64. The scatter diagrams for SISO-OFDM systems show a phase rotation due to the CPE and the ICI noise around the signal points. From the figure, we can see that the constellation rotation in the

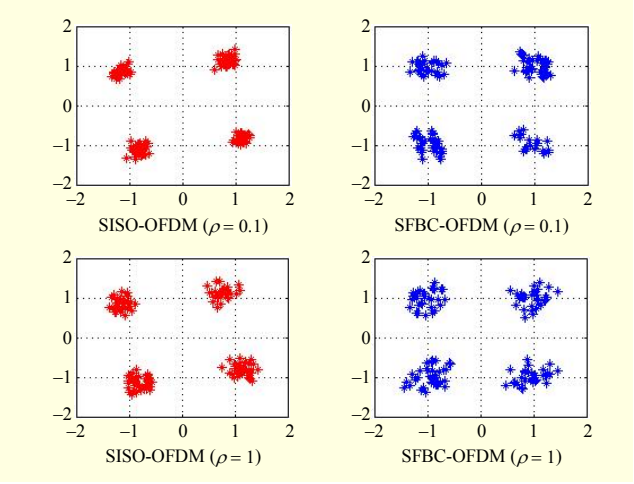

Fig. 2. Scatter diagrams of a SISO-OFDM system and a conventional Alamouti SFBC-OFDM system with PHN and RCFO ε = 0.05.

conventional SFBC-OFDM systems is less than that in SISO-OFDM systems, but the signal of the former is more dispersed than that of SISO-OFDM systems due to the effect of ICI.

III. Proposed ISC Scheme for Alamouti SFBC-OFDM System

To efficiently cancel out the ICI caused by PHN and RCFO, we propose a new ISC method for Alamouti SFBC-OFDM systems. Figure 3 shows a baseband model of the Alamouti SFBC-OFDM system with the proposed ISC method. In the figure, a new ICI cancelling modulation (ICM) and ICI cancelling demodulation (ICD) are used for the purpose of the ISC.

The Alamouti SFBC signal $S_{k,i}$, for $i = 1, 2$, and $k = 0, 2, 4, \ldots, N/2-1$, for the TX1 and TX2 is given by

$$\begin{aligned} &\text{TX1}: \; S_{k,1} = X_k, \;\; S_{k+1,1} = X_{k+1}, \\ &\text{TX2}: \; S_{k,2} = -X_{k+1}^*, \;\; S_{k+1,2} = X_k^*. \end{aligned} \tag{14}$$

The proposed ISC method is as follows. The symbol $V_{k,i}$ after applying a new ICM is given by

$$V_{k,i} = \begin{cases} \text{Re}(S_{0,i}) & k = 0, \\ \text{Im}(S_{0,i}) & k = N/2, \\ S_{k,i} & 1 \le k \le N/2-1, \\ S_{N-k,i}^* & N/2 \le k < N-1, \end{cases} \tag{15}$$

which can be rewritten in vector form as follows:

$$\begin{aligned} \mathbf{V}_1 &= [V_{0,1}, V_{1,1}, \ldots, V_{N-1,1}] \\ &= [\text{Re}(S_{0,1}), S_{1,1}, \ldots, S_{N/2-2,1}, S_{N/2-1,1}, \\ &\qquad \text{Im}(S_{0,1}), S_{N/2-1,1}^*, \ldots, S_{2,1}^*, S_{1,1}^*] \\ &= [\text{Re}(X_0), X_1, \ldots, X_{N/2-2}, X_{N/2-1}, \\ &\qquad \text{Im}(X_0), X_{N/2-1}^*, \ldots, X_2^*, X_1^*], \end{aligned} \tag{16}$$

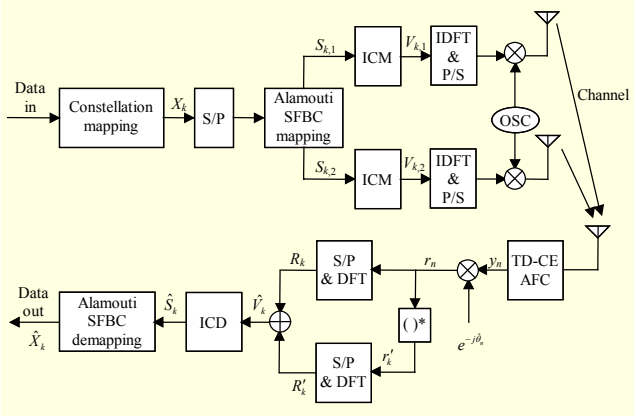

Fig. 3. Block diagram of Alamouti SFBC-OFDM system with proposed ISC.

$$\begin{aligned} \mathbf{V}_2 &= [V_{0,2}, V_{1,2}, \ldots, V_{N-1,2}] \\ &= [\text{Re}(S_{0,2}), S_{1,2}, \ldots, S_{N/2-2,2}, S_{N/2-1,2}, \\ &\qquad \text{Im}(S_{0,2}), S_{N/2-1,2}^*, \ldots, S_{2,2}^*, S_{1,2}^*] \\ &= [\text{Re}(-X_1^*), X_0^*, \ldots, -X_{N/2-1}^*, X_{N/2-2}^*, \\ &\qquad \text{Im}(-X_1^*), X_{N/2-2}, \ldots, -X_3, X_0], \end{aligned} \tag{17}$$

where $\mathbf{V}_1$ and $\mathbf{V}_2$ are the SFBC-OFDM transmit symbols for TX1 and TX2, respectively.

By performing IDFTs on $\mathbf{V}_1$ and $\mathbf{V}_2$, the time-domain transmit signal can be written as

$$\begin{aligned} v_{n,i} &= \frac{1}{N}\sum_{m=0}^{N-1} V_{m,i} e^{j2\pi nm/N}, \quad 0 \le n < N, \;\; i = 1, 2, \\ &= \frac{1}{N}(V_{0,i} + V_{N/2,i} e^{j2\pi n(N/2)/N}) \\ &\quad + \frac{1}{N}\sum_{m=0}^{N/2-1} (V_{m,i} e^{j2\pi nm/N} + V_{N-m,1} e^{j2\pi n(N-m)/N}). \end{aligned} \tag{18}$$

From (16) and (17), $v_{n,i}$ can be rewritten as

$$\begin{aligned} v_{n,i} &= \frac{1}{N}(\text{Re}(S_{0,i}) + \text{Im}(S_{0,i})(-1)^n) \\ &\quad + \frac{1}{N}\sum_{m=0}^{N/2-1} (S_{m,i} e^{j2\pi nm/N} + S_{m,i}^* e^{-j2\pi nm/N}) \\ &= \frac{1}{N}(\text{Re}(S_{0,i}) + \text{Im}(S_{0,i})(-1)^n) \\ &\quad + \frac{1}{N}\sum_{m=0}^{N/2-1} 2\,\text{Re}(S_{m,i} e^{j2\pi nm/N}). \end{aligned} \tag{19}$$

From (19), we can observe that the transmit signal $v_{n,i}$ is a real-valued signal.

At the receiver shown in Fig. 3, the received signal passes through the time-domain channel estimator (TD-CE) and auto frequency control (AFC). Joint estimation of carrier frequency offset (CFO) and channel impulse response for OFDM systems with PHN are discussed in [22]. Although the channel estimator estimates the Doppler frequency and channel impulse response and the AFC estimates and compensates the CFO, there still exist an RCFO and a PHN due to the estimation error.

The received signal is influenced by the PHN and RCFO and can be written as

$$y_n = (v_{n,1} + v_{n,2}) e^{j\theta_n} + w_n, \quad 0 \le n < N, \tag{20}$$

where θ_n is given by $\theta_n = \phi_n + 2\pi n\varepsilon / N$, ϕ_n is PHN, ε is a normalized frequency offset, and w_n is an AWGN with a mean of zero and a variance of $\sigma_w^2 = N_0/2$. Because the local oscillator is phase locked and an initial frequency offset acquisition is made by means of the AFC, we can assume that $\theta_n \ll \pi/2$.

Since $v_{n,1} + v_{n,2}$ is a real value, we can blindly estimate θ_n

http://dx.doi.org/10.4218/etrij.14.0113.0711

from y_n as follows:

$$\hat{\theta}_n = \angle y_n, \tag{21}$$

where $\angle$ denotes the argument of a complex number.

Then the phase offset caused by PHN and RCFO is compensated in the proposed scheme. The phase offset compensated signal is given by

$$r_n = y_n e^{-j\hat{\theta}_n} = (v_{n,1} + v_{n,2}) e^{j\tilde{\theta}_n} + w'_n, \quad 0 \le n < N, \tag{22}$$

where $\tilde{\theta} = \theta_n - \hat{\theta}_n$.

After applying the DFT operation to r_n, the DFT output in the upper path shown in Fig. 3 can be written as

$$R_k = \sum_{m=0}^{N-1} (V_{m,1} + V_{m,2}) \tilde{\Theta}_{k-m} + W_k, \quad 0 \le k \le N-1, \tag{23}$$

where $\tilde{\Theta}_{k-m}$ is given by

$$\tilde{\Theta}_{k-m} = \frac{1}{N} \sum_{n=0}^{N-1} e^{j\tilde{\theta}_n} e^{-j2\pi n(k-m)/N}. \tag{24}$$

Similarly, the DFT output in the lower path can be written as

$$R'_k = \sum_{m=0}^{N-1} (V_{m,1} + V_{m,2}) \tilde{\Theta}^*_{-(k-m)} + W^*_k, \quad 0 \le k \le N-1. \tag{25}$$

Then the ISC demodulated signal is given by

$$\begin{aligned} \hat{V}_k &= \frac{R_k + R'_k}{2} \\ &= \frac{1}{2}(V_{k,1} + V_{k,2})(\tilde{\Theta}_0 + \tilde{\Theta}^*_0) \\ &\quad + \frac{1}{2} \sum_{\substack{m=0 \\ m \ne k}}^{N-1} (V_{m,1} + V_{m,2})(\tilde{\Theta}_{k-m} + \tilde{\Theta}^*_{-(k-m)}) + \mathrm{Re}[W_k]. \end{aligned} \tag{26}$$

Due to the symmetric conjugate property of $\tilde{\Theta}_k$, the proposed ISC scheme can eliminate the CPE and ICI efficiently. Using $\hat{V}_k$, Alamouti SFBC-OFDM symbols can be estimated as follows:

$$\hat{S}_0 = \mathrm{Re}\{\hat{V}_0\} + j\,\mathrm{Re}\{\hat{V}_{N/2}\} \approx S_{0,1} + S_{0,2} = X_k - X^*_{k+1}, \tag{27}$$

$$\hat{S}_k = \frac{\hat{V}_k + \hat{V}^*_{N/2}}{2} \approx S_{k,1} + S_{k,2} = X_{k+1} + X^*_k, \quad 1 \le k \le (N/2)-1. \tag{28}$$

To detect $\hat{X}_k$ and $\hat{X}_{k+1}$, $k = 0, 2, 4, \ldots, (N/2)-2$, $\hat{S}_k$ and $\hat{S}_{k+1}$ are combined in a way similar to that done in an SFBC de-mapping and are given by

$$\hat{X}_k = \frac{\hat{S}_k + \hat{S}^*_{k+1}}{2}, \quad \hat{X}_{k+1} = \frac{\hat{S}_{k+1} - \hat{S}^*_k}{2}. \tag{29}$$

The average CIR of the proposed scheme at the kth subcarrier can easily be shown to be

$$CIR_{\mathrm{pro}} = \frac{|\tilde{\Theta}_0 + \tilde{\Theta}^*_0|^2}{\sum_{m=1}^{N-1} |\tilde{\Theta}_{-m} + \tilde{\Theta}^*_m|^2}. \tag{30}$$

IV. Simulation Results

In this section, we compare the effect of PHN and RCFO on the performance of the proposed and conventional schemes: (a) a SISO-OFDM system without ISC (16 QAM), (b) an Alamouti SFBC-OFDM system without ISC (32 QAM), and (c) an Alamouti SFBC-OFDM system with the conventional symmetric ISC (64 QAM) [15].

The modulation order has been differently selected for each scheme to make the bandwidth efficiency of all schemes equal to 1 bit/Hz/s.

The same value of E_b / N_0 (the ratio of the signal energy per information bit to noise power spectral density) has been used to examine the BER performance, which yields a fair comparison among the proposed scheme and the three conventional schemes.

PHN is randomly generated as independent and identically distributed Gaussian samples with the following power spectral density (PSD), $L(f)$, [12]

$$L(f) = \begin{cases} 10^{-a} & 0 \le |f| \le \beta, \\ 10^{-a} \left(\frac{f}{\beta}\right)^{-b} & \beta \le |f| \le \gamma, \\ 10^{-c} & \gamma \le |f| \le f_s/2, \end{cases} \tag{31}$$

where $a = 6.5$, $b = 2$, $c = 12$, and γ =100 MHz. The parameter β is the 3 dB bandwidth of the PSD, and f_s is the sampling rate.

The total number of subcarriers is 128, and the propagation channel model is the Extended Pedestrian A (EPA) model of which its parameters are described in Table 1 [23]. The channel

Table 1. EPA channel model.

Tap	Relative delay (nsec)	Average power (dB)
1	0	0
2	30	–1.0
3	70	–2.0
4	90	–3.0
5	110	–8.0
6	190	–17.2
7	410	–20.8

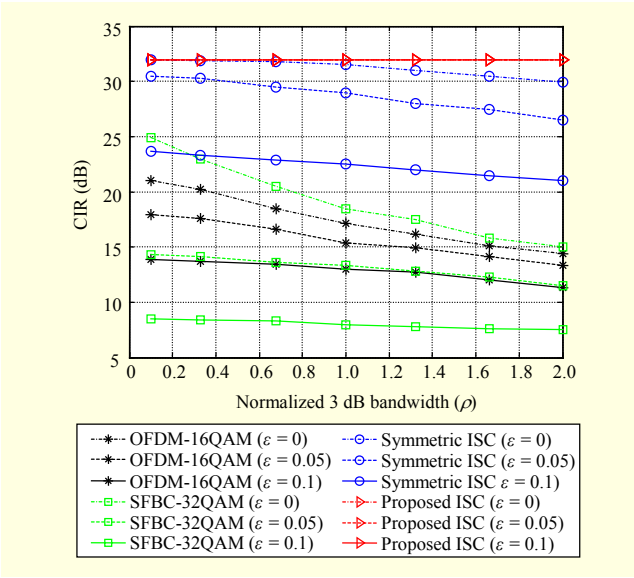

Fig. 4. Average CIR vs. normalized 3 dB bandwidth of PHN (ρ).

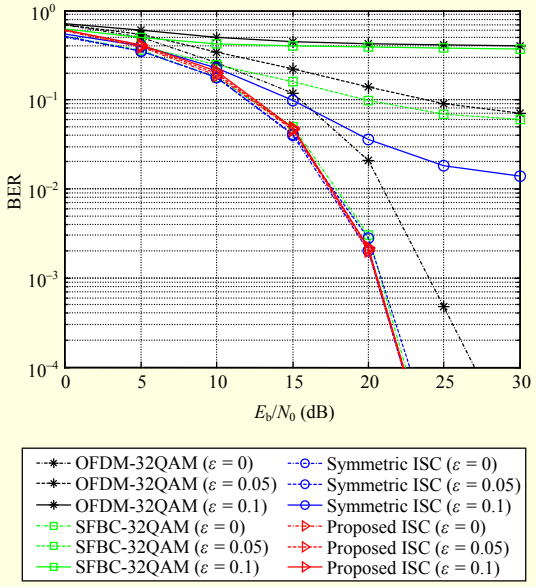

Fig. 5. BER comparison when $\rho = 0.1$.

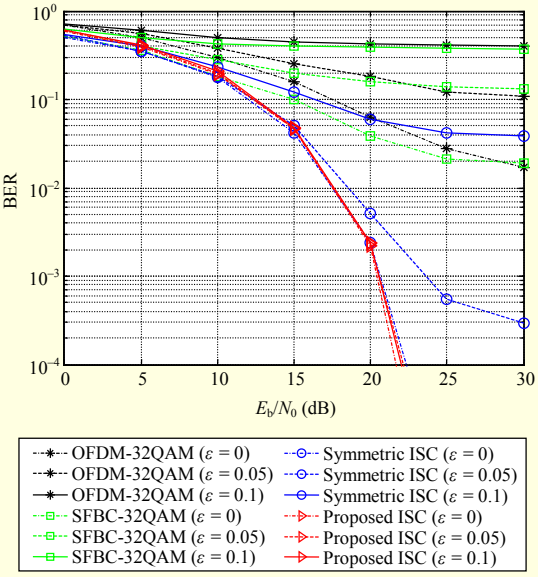

Fig. 6. BER comparison when $\rho = 1$.

estimation is assumed to be perfect, and the channel is equalized using a zero-forcing algorithm. The CFO offset is initially compensated by the AFC; therefore, we consider only the RCFO.

Figure 4 shows the CIR performance comparison of the SISO-OFDM system without ISC, Alamouti SFBC-OFDM system with and without the conventional ISC [15], and the proposed scheme. In the figure, "OFDM-16 QAM," "SFBC-32 QAM," "Symmetric ISC," and "Proposed ISC" represent the SISO-OFDM system without ISC, Alamouti SFBC-OFDM system without ISC, Alamouti SFBC-OFDM system with conventional ISC, and the proposed scheme, respectively. We can observe that the Alamouti SFBC-OFDM system has better CIR performance than the SISO-OFDM system when $\varepsilon = 0$ and $\rho < 1$ owing to the diversity gain. However, the performance of the former is worse than that of the SISO-OFDM system as the values of ρ and ε become larger. This is because the orthogonal property between subcarriers is severely destroyed and thus causes ICI to increase. We can also observe that the proposed scheme has better CIR performance than the SFBC-OFDM system with the conventional ISC method, especially when $\rho > 0.8$ or there exists RCFO. This is because PHN and RCFO can be blindly estimated and compensated at the receiver using the real property of the transmit signals in the proposed scheme.

Figures 5, 6, and 7 show the BER performance of the conventional schemes and the proposed scheme for $\rho = 0.1$, 1, and 2, respectively. From the figures, we can observe that when the values of ρ and ε are small, the BER performance of the Alamouti SFBC-OFDM system is better than that of the SISO-OFDM system because of the diversity gain. However, as ρ and ε become large, the BER performance of the former is worse than that of the SISO-OFDM system; that is, the Alamouti SFBC-OFDM system does not have diversity gain. In the case of symmetric ISC, its BER performance is much better that that of the SISO-OFDM system when $\rho < 1$ and $\varepsilon < 0.05$; however, it becomes worse when $\rho \geq 1$ and $\varepsilon > 0.05$, as in the SISO-OFDM system. We can also observe that the BER performance of the

http://dx.doi.org/10.4218/etrij.14.0113.0711

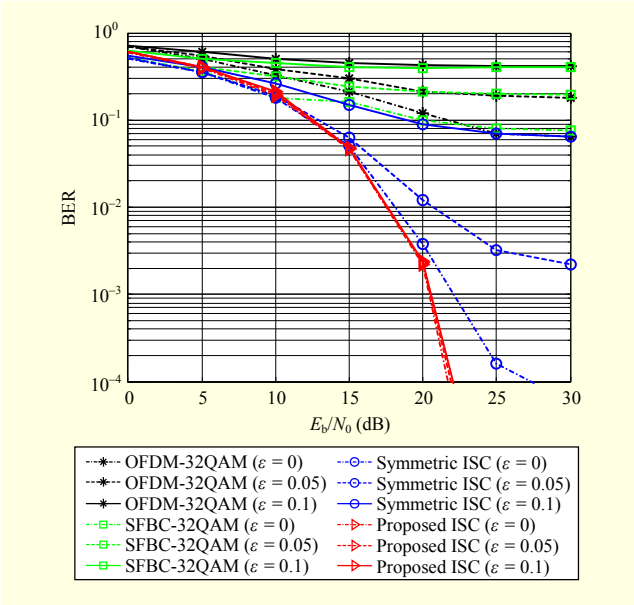

Fig. 7. BER comparison when $\rho = 2$.

proposed scheme is better than that of the SFBC-OFDM system with the conventional ISC method, especially when ρ is large or there exists RCFO. This is because PHN and RCFO can be blindly estimated and compensated at the receiver using the real property of the transmit signals in the proposed scheme.

V. Conclusion

In this paper, we analyzed the effect of PHN and RCFO on the performance of the conventional Alamouti SFBC-OFDM system. Since the conventional SFBC-OFDM system suffers severely due to PHN and RCFO, we proposed a new ICI suppression scheme for SFBC-OFDM systems. Through the simulation results, we showed that the proposed scheme has better performance compared to conventional schemes, especially when the normalized 3 dB bandwidth (ρ) of the PHN is large or there exists RCFO.

Appendix. Derivation of (10)

The ICI power of the conventional SFBC-OFDM system at the 0th subcarrier is given by

$$ICI_{\text{SFBC}} = \frac{1}{4} E[|\,(\Theta_{-\varepsilon} - \Theta^*_{-\varepsilon}) X_1^* + I_{0,1} + I_{1,1}^* + I_{0,2} + I_{1,2}^*\,|^2]. \quad (32)$$

Using the property $E[X_m^2] = 0$ and the independence condition of X_m for $m = 0, 1, \ldots, N-1$, ICI_{SFBC} becomes

$$\begin{aligned} ICI_{\text{SFBC}} = \frac{1}{4} E[| & \sum_{m=2,4,\ldots}^{N-2} (\Theta_{-m-\varepsilon} + \Theta^*_{-m-\varepsilon}) X_m \\ & + \sum_{m=0,2,4,\ldots}^{N-2} \{(\Theta_{-(m+1+\varepsilon)} + \Theta^*_{-(m-1+\varepsilon)}) X_m^* \\ & + (\Theta_{-(m+1+\varepsilon)} + \Theta^*_{-(m-1+\varepsilon)}) X_{m+1} \\ & - (\Theta_{-m-\varepsilon} - \Theta^*_{-m-\varepsilon}) X_{m+1}^* \}\,|^2]. \end{aligned} \quad (33)$$

It can be written as

$$\begin{aligned} ICI_{\text{SFBC}} = & \frac{1}{4} \sum_{m=2,4,\ldots}^{N-2} |\,\Theta_{-m-\varepsilon} - \Theta^*_{-m-\varepsilon}\,|^2 \\ & + \frac{1}{4} \sum_{m=0,2,4,\ldots}^{N-2} \{|\,\Theta_{-(m+1+\varepsilon)} + \Theta^*_{-(m-1+\varepsilon)}\,|^2 \\ & + |\,\Theta_{-(m+1+\varepsilon)} + \Theta^*_{-(m-1+\varepsilon)}\,|^2 \\ & + |\,\Theta_{-m-\varepsilon} - \Theta^*_{-m-\varepsilon}\,|^2\} \\ = & \frac{1}{4} |\,\Theta_{-\varepsilon} - \Theta^*_{-\varepsilon}\,|^2 \\ & + \frac{1}{2} \sum_{m=2,4,\ldots}^{N-2} \{|\,\Theta_{-m-\varepsilon}\,|^2 + |\,\Theta^*_{-m-\varepsilon}\,|^2\} \\ & + \frac{1}{2} \sum_{m=0,2,4,\ldots}^{N-2} \{|\,\Theta_{-(m+1+\varepsilon)}\,|^2 + |\,\Theta^*_{-(m-1+\varepsilon)}\,|^2\}. \end{aligned} \quad (34)$$

Because $\Theta_1 = \Theta_{-(N-1)}$ and $|\,\Theta_{-l}\,|^2 = |\,\Theta^*_{-l}\,|^2$, the third term of (34) becomes

$$\begin{aligned} & \frac{1}{2} \sum_{m=0,2,4,\ldots}^{N-2} \{|\,\Theta_{-(m+1+\varepsilon)}\,|^2 + |\,\Theta^*_{-(m-1+\varepsilon)}\,|^2\}, \\ & = \frac{1}{2} |\,\Theta^*_{1-\varepsilon}\,|^2 + \sum_{m=1,3,5,\ldots}^{N-2} |\,\Theta_{-m+\varepsilon}\,|^2 + \frac{1}{2} |\,\Theta_{-(N-1+\varepsilon)}\,|^2 \\ & = \sum_{m=1,3,5,\ldots}^{N-1} |\,\Theta_{-m-\varepsilon}\,|^2 . \end{aligned} \quad (35)$$

Therefore, we finally obtain

$$ICI_{\text{SFBC}} = \frac{1}{4} |\,\Theta_{-\varepsilon} - \Theta^*_{-\varepsilon}\,|^2 + \sum_{m=1}^{N-1} |\,\Theta_{-m-\varepsilon}\,|^2 . \quad (36)$$

References

[1] ETSI, Tech. Report ETS 300 401, "*Radio Broadcasting System: Digital Audio Broadcasting (DAB) to Mobile, Portable and Fixed Receivers*," Aug. 1997.

[2] ETSI, Tech. Report ETS 300 744, "*Digital Video Broadcasting (DVB): Framing Structure, Channel Coding and Modulation for Digital Terrestrial Television*," Aug. 1997.

[3] K. Sistanizadeh, P.S. Chow, and J.M. Cioffi, "Multi-tone Transmission for Asymmetric Digital Subscriber Lines (ADSL)," *IEEE Int. Conf. Commun.*, Geneva, Switzerland, vol. 2, May 23–26, 1993, pp. 756–760.

[4] IEEE Standard 802.11a, "*Wireless LAN Medium Access Control*

(MAC) and Physical Layer (PHY) Specification," June 1999.

[5] R. Nee and R. Prasad, *OFDM for Wireless Multimedia Communications*, Norwood, MA: Artech House Publishers, 2000.

[6] D.-B. Lin, P.-H. Chiang, and H.-J. Li, "Performance Analysis of Two-Branch Transmit Diversity Block-Coded OFDM Systems in Time-Varying Multipath Rayleigh-Fading Channels," *IEEE Trans. Veh. Technol*., vol. 54, no. 1, Jan. 2005, pp. 136–148.

[7] J. Kim, R.W. Heath, and E.J. Powers, "Receiver Designs for Alamouti Coded OFDM Systems in Fast Fading Channels," *IEEE Trans. Wireless Commun*., vol. 4, no. 2, Mar. 2005, pp. 550–559.

[8] Y. Gong and K.B. Letaief, "An Efficient Space-Frequency Coded OFDM System for Broadband Wireless Communications," *IEEE Trans. Commun*., vol. 51, no. 12, Dec. 2003, pp. 2019–2029.

[9] S. Alamouti, "A Simple Transmit Diversity Technique for Wireless Communications," *IEEE J. Sel. Areas Commun*., vol. 16, no. 8, Oct. 1998, pp. 1451–1458.

[10] A.G. Armada, "Understanding the Effects of Phase Noise in Orthogonal Frequency Division Multiplexing (OFDM)," *IEEE Trans. Broadcast*., vol. 47, no. 2, June 2001, pp. 153–159.

[11] M.S. El-Tanany, Y. Wu, and L. Hazy, "Analytical Modeling and Simulation of Phase Noise Interference in OFDM-Based Digital Television Terrestrial Broadcasting Systems," *IEEE Trans. Broadcast*., vol. 47, no. 1, Mar. 2001, pp. 20–31.

[12] P. Robertson and S. Kaiser, "Analysis of the Effects of Phase-Noise in Orthogonal Frequency Division Multiplex (OFDM) Systems," *IEEE Int. Conf. Commun*., Seattle, WA, USA, vol. 3, June 18–22, 1995, pp. 1652–1657.

[13] Z. Jianhua, H. Rohling, and Z. Ping, "Analysis of ICI Cancellation Scheme in OFDM Systems with Phase Noise," *IEEE Trans. Broadcast*., vol. 50, no. 2, June 2004, pp. 97–106.

[14] H.-G. Ryu, Y. Li, and J.-S. Park, "An Improved ICI Reduction Method in OFDM Communication Systems," *IEEE Trans. Broadcast*., vol. 51, no. 3, Sept. 2005, pp. 395–400.

[15] S. Tang et al., "Inter-carrier Interference Cancellation with Frequency Diversity for OFDM Systems," *IEEE Trans. Broadcast*., vol. 53, no. 1, Mar. 2007, pp. 132–137.

[16] J. Tubbax et al., "Compensation of IQ Imbalance and Phase Noise in OFDM Systems," *IEEE Trans. Wireless Commun*., vol. 4, no. 3, May 2005, pp. 872–877.

[17] Q. Zou, A. Tarighat, and A.H. Sayed, "Compensation of Phase Noise in OFDM Wireless Systems," *IEEE Trans. Signal Process*., vol. 55, no. 11, Nov. 2007, pp. 5407–5424.

[18] D. Petrovic, W. Rave, and G. Fettweis, "Effects of Phase Noise on OFDM Systems with and without PLL: Characterization and Compensation," *IEEE Trans. Commun*., vol. 55, no. 8, Aug. 2007, pp. 1607–1616.

[19] R. Yang and R.S. Sherratt, "Enhancing MB-OFDM Throughput with Dual Circular 32-QAM," *IEEE Trans. Consum. Electron*., vol. 54, no. 4, Nov. 2008, pp. 1640–1646.

[20] J. Park et al., "An Enhanced Dual Carrier Modulation for Performance Improvement in WiMedia UWB Systems," *IEEE Trans. Consum. Electron*., vol. 57, no. 4, Nov. 2011, pp. 1556–1563.

[21] S. Lu, B. Narasimhan, and N. Al-Dhahir, "A Novel SFBC-OFDM Scheme for Doubly Selective Channels," *IEEE Trans. Veh. Technol*., vol. 58, no. 5, June 2009, pp. 2573–2578.

[22] J. Tao, J. Wu, and C. Xiao, "Estimation of Channel Transfer Function and Carrier Frequency Offset for OFDM Systems with Phase Noise," *IEEE Trans. Veh. Technol*., vol. 58, no. 8, Oct. 2009, pp. 4380–4387.

[23] 3GPP Technical Specification, TS 36.101 V11.6.0, *User Equipment (UE) Radio Transmission and Reception,* Sept. 2013.

Kyung-Hwa Kim received her BS degree in electrical engineering from Ewha Womans University, Seoul, Rep. of Korea, in 2000 and her MS and PhD degrees in electrical engineering in 2002 and 2011, both from Korea Advanced Institute of Science and Technology, Daejeon, Rep. of Korea. Since 2010, she has been a researcher with LG Electronics, Seoul, Rep. of Korea. Her research interests include broadband wireless communication systems, MIMO systems, and the development of modem algorithms for communication systems such as LTE and WCDMA.

Bangwon Seo received his BS, MS, and PhD degrees in electrical engineering from Korea Advanced Institute of Science and Technology, Daejeon, Rep. of Korea, in 1997, 1999, and 2010, respectively. From November 2004 to February 2013, he was with the Electronics and Telecommunications Research Institute, Department, Rep. of Korea. In March 2013, he joined the Division of Electrical, Electronic and Control Engineering, Kongju National University, Cheonan, Rep. of Korea, where he is currently an assistant professor. His research interests include receiver design, OFDM systems, MIMO systems, massive MIMO, CoMP, device-to-device direct communications, MC-CDMA systems, and cognitive radio networks.